ORNL/TM-13252

ornl

OAK RIDGE NATIONAL LABORATORY

LOCKHEED MARTIN

Configuration Studies for a Small-Aspect-Ratio Tokamak-Stellarator Hybrid

B. A. Carreras
V. E. Lynch
A. Ware

MANAGED AND OPERATED BY
LOCKHEED MARTIN ENERGY RESEARCH CORPORATION
FOR THE UNITED STATES
DEPARTMENT OF ENERGY

ORNL-27 (3-96)

RB

ORNL/TM-13252
Dist. Category UC-427

Fusion Energy Division

CONFIGURATION STUDIES FOR A SMALL-ASPECT-RATIO TOKAMAK STELLARATOR HYBRID

B. A. Carreras
V. E. Lynch
A. Ware

Date Published—August 1996

Prepared by
OAK RIDGE NATIONAL LABORATORY
managed by
LOCKHEED MARTIN ENERGY RESEARCH CORPORATION
for the
U.S. DEPARTMENT OF ENERGY
under Contract No. DE-AC05-96OR22464

CONTENTS

LIST OF FIGURES

CONFIGURATION STUDIES FOR A SMALL-ASPECT-RATIO TOKAMAK-STELLARATOR HYBRID

B. A. Carreras
V. E. Lynch
A. Ware

ABSTRACT

The use of modulated toroidal coils offers a new path to the tokamak-stellarator hybrids. Low-aspect-ratio configurations can be found with robust vacuum flux surfaces and rotational transform close to the transform of a reverse-shear tokamak. These configurations have clear advantages in minimizing disruptions and their effects and in reducing tokamak current drive needs. They also allow the study of low-aspect-ratio effects on stellarator confinement in small devices.

1. INTRODUCTION

Tokamaks have made tremendous progress in pushing fusion-relevant parameters closer to the reactor goals. Because they are the best studied magnetic configurations, tokamaks are primary candidates for the fusion reactor. However, they have an intrinsic flaw, the disruptive instability. Present tokamaks can be operated with a very low risk of disruption, but never a zero risk. A fusion reactor will be operated in an environment very different from that of present experiments, and the potential for disruption will remain a major operational problem. Many of the critical issues for existing configurations have an economic impact on the reactor. They are amenable to trade-off. However, the disruption problem has not only an economic impact but an impact on safety as well. This is a serious vulnerability for the tokamak concept.

Stellarators have the advantage of zero-current operation. This eliminates de facto the disruption instability. However, low aspect ratio presents many problems to those configurations. First, magnetic surfaces are fragile, and techniques for control of the magnetic surfaces need to be developed.[1] On the other hand, the reduction of collisionless losses also pushes the configurations toward a high aspect ratio. The result is that all present designs have a large aspect ratio ($A > 5$), and they lead to very large reactors. In our Compact Torsatron optimization studies, we were not able to identify configurations with an aspect ratio below 3.

It would be desirable to make use of most tokamak advantages and at the same time eliminate the disruption problem. To do so, we have investigated magnetic configurations with an external rotational transform that is tokamaklike. These configurations can operate as tokamak-stellarator hybrids without the disadvantages of having to greatly modify the rotational transform and cross the $q = 2$ surface. The existence of vacuum flux surfaces provides confinement without current. Small amounts of current can be driven to better control the configuration at finite beta. We have studied low-aspect-ratio configurations, close to the usual tokamak aspect ratios. Because these configurations have a rotational transform below 0.25, no low-resonant surfaces contribute to the fragility of vacuum flux surfaces. The issue of low collisionality losses is present for the currentless operation. However, the recent experience with tokamaks has taught us to use radial electric field shear barriers to eliminate anomalous transport and reduce neoclassical losses. This approach must be investigated as an alternative to the quasi-symmetric stellarators.

The remainder of the paper is organized as follows. In Sect. 2, the coil parameterization is discussed, and in Sect. 3 the main physics properties of the vacuum field

configurations are presented. The configurations presented here may have large magnetic field ripple; ways of reducing the ripple are studied in Sect. 4. Finally, the conclusions are presented in Sect. 5.

2. MODULATED TOROIDAL COILS

The use of twisted toroidal coils to provide an additional rotational transform to tokamaks was first proposed by H. Furth and collaborators.[2] Studies of this configuration did not lead to resilient flux surfaces.[3] Tilted toroidal coils have also been proposed as a way of generating rotational transform.[4,5] We have used a similar approach by giving a modulation to a set of toroidal field coils. This modulation enabled us to go to lower aspect ratio and have more flexible control of the transform and ripple.

For a configuration with M toroidal field periods and N coils per field period, we describe the coil i by a filament with these coordinates:

$$X_i = X_{i0} + \frac{1}{e_i} R_i \cos(\Phi_i) , \tag{1}$$

$$Y_i = Y_{i0} + \frac{1}{e_i} R_i \sin(\Phi_i) , \tag{2}$$

$$Z_i = e_i R_0 \sin(\theta) , \tag{3}$$

where θ is a continuous parameter defined between π and $-\pi$. The toroidal angle Φ_i in Eqs. (1) and (2) is given in terms of the parameter θ by

$$\Phi_i = \hat{\Phi}_i - p_i[\theta - \alpha_i \sin(\theta) - \beta_{1i} \sin(2\theta) - \beta_{2i} \sin(3\theta) - \beta_{3i} \sin(4\theta)] , \tag{4}$$

with $\hat{\Phi}_i = 2\pi i / N_c$, N_c the total number of coils, R_0 the radius of the coils, α_i and β_{ji} (j = 1,2,3) the usual coil modulation parameters, and

$$R_i = R_0\{1 - \delta_{Ti} + [1 + \delta_{Ti} \cos(\theta)]\cos(\theta)\} . \tag{5}$$

The displacement of the coils is given by

$$X_{i0} = \delta_i \cos\left(\hat{\Phi}_i\right),$$

$$Y_{i0} = \delta_i \sin\left(\hat{\Phi}_i\right). \tag{6}$$

The main coil cross-section shape parameters, ellipticity (e_i), pitch (p_i), and triangularity (δ_{Ti}) are also functions of the coil position, but they maintain the symmetry of the field period.

A typical set of modulated coils for an $M = 4$ configuration with one coil per field period is shown in Fig. 1. This parameterization of the coils has allowed us to explore a broad range of configurations. To control the plasma size in some of the configurations

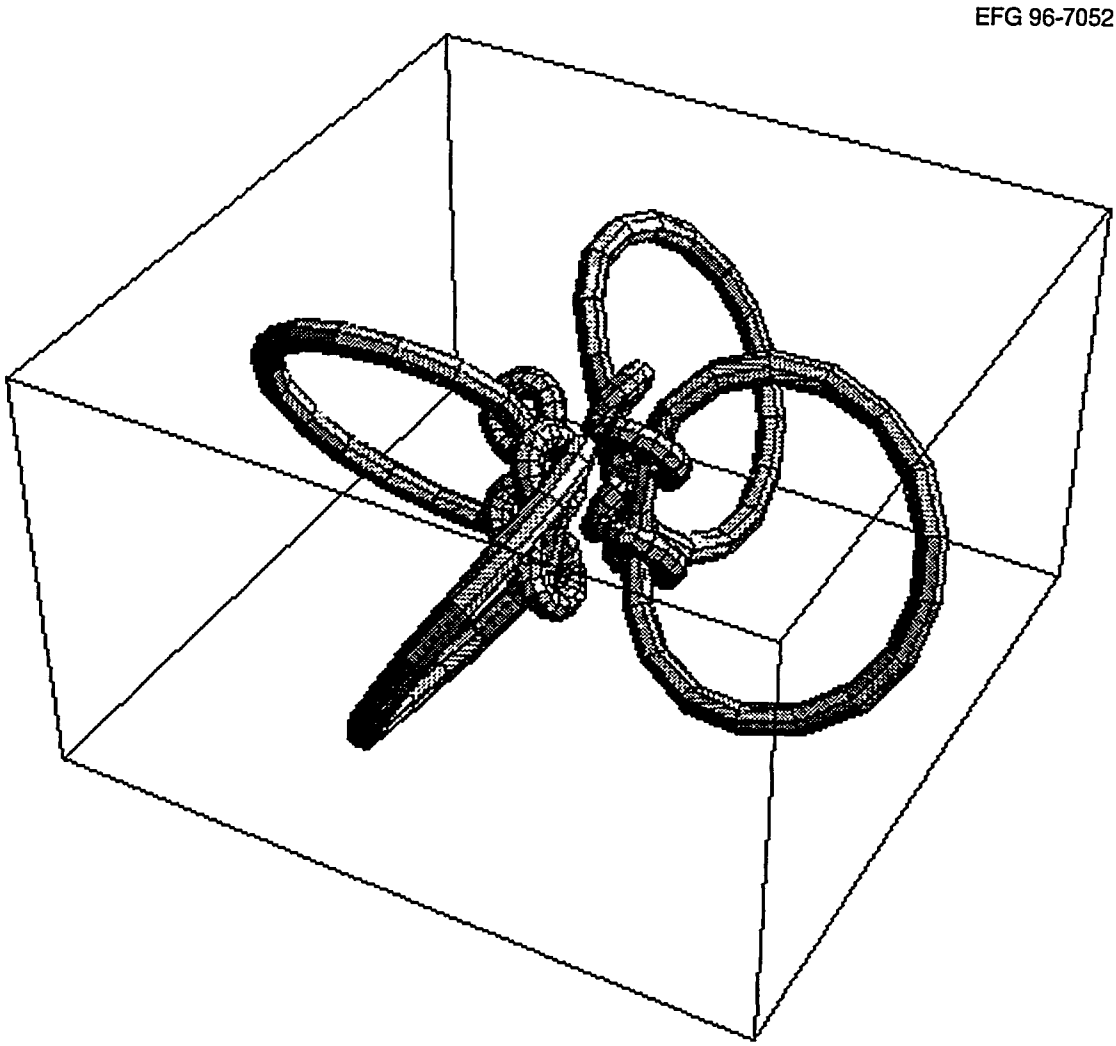

Fig. 1. Set of coils for the $M = 4$ configuration.

studied, it has been useful to add small modulated coils with the opposite pitch to the large coils (Fig. 2). The size-control coils help in changing the utilization size and in defining the location of the X-points that can be used for divertor purposes.

Additional poloidal field coils are needed to control the position of the magnetic axis and can also be used to modify the rotational transform.[6]

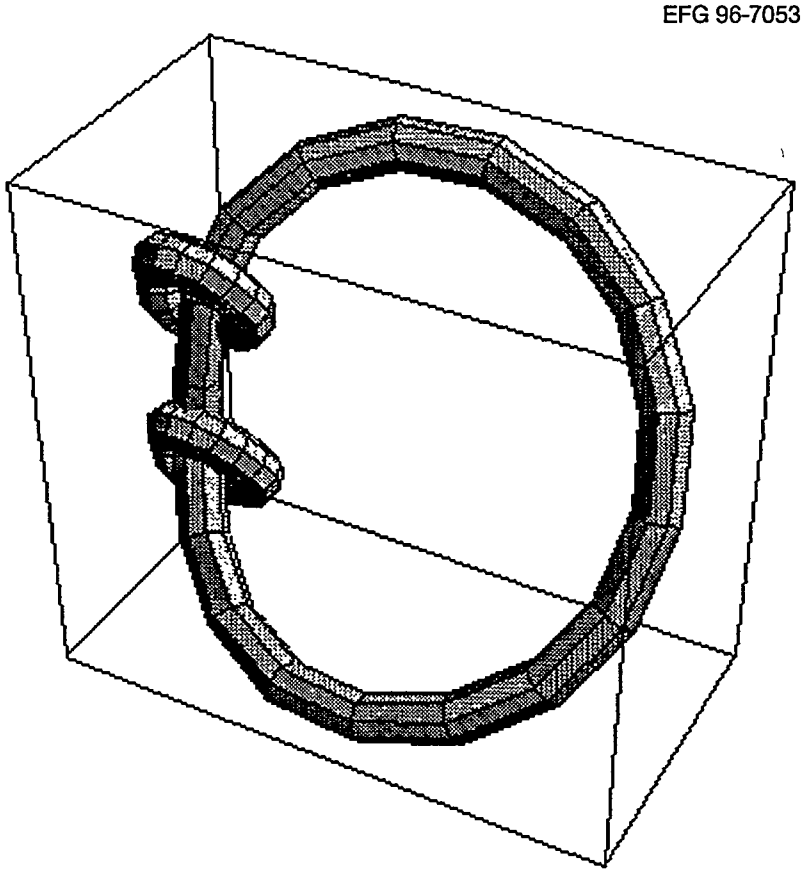

Fig. 2. Individual toroidal modulated coil with two size control coils.

3. MAIN PHYSICS PROPERTIES OF THE VACUUM CONFIGURATIONS

There are two main target parameters in the vacuum field configuration studies: the rotational transform at the magnetic axis about 0.2 and the aspect ratio below 2.5. The aspect ratio is understood in the stellarator sense; $A \equiv \langle R_{axis} \rangle / \langle a \rangle$, where $\langle R_{axis} \rangle$ is the toroidal angle average of the magnetic axis position and $\langle a \rangle$ the average minor radius.

We first considered configurations having from three to six field periods with a single coil per field period and circular cross-section coils. As the number of field periods increases, it becomes more difficult to find vacuum configurations with the prescribed aspect ratio. The $M = 4$ configuration was taken as a reference case for this family of configurations, and it is a good example of their characteristic properties.

The $M = 4$ configuration has good flux surfaces with a vacuum utilization volume of aspect ratio $A = 2.0$. This is the lowest-aspect-ratio configuration achieved with external coils in our studies. The vacuum magnetic flux surfaces (Fig. 3) are characterized by having two almost axisymmetric X-points inside. The X-points correspond to the $\iota = 0$ surface; therefore, the last flux surface has the characteristic properties of the tokamak separatrix and offers the possibility of having a tokamaklike divertor. The role of the size-control coils (Fig. 2) is important in increasing the overall volume and controlling the position of the X-points.

The $M = 4$ configuration is a good test bed for a hybrid tokamak-stellarator. The main reason is that its rotational transform is tokamaklike. In Fig. 4, the rotational transform for this configuration is compared to the transform of a typical reversed-shear tokamak configuration. Only a small additional toroidal current is needed to reach the tokamak q-profile. Furthermore, the additional current does not take the rotational transform across the $q = 2$ surface as it would be the case for standard stellarators. For most stellarators, the rotational transform either crosses $\iota = 0.5$ or stays above (Fig. 5). They also have the opposite edge shear to a tokamak. Therefore, what was considered a critical drawback of the standard tokamak-stellarator hybrids[7] has been eliminated. To have the same transform as a tokamak, a relatively low toroidal current, peaked at about one-half of the plasma minor radius, must be driven. This offers a very favorable current drive scenario.

The averaged magnetic field line curvature is favorable. The calculated V' is negative over the whole volume and remains negative when the magnetic axis is shifted in or out. This contrasts with the torsatron configurations that are characterized by a strong magnetic hill at the edge. This is shown in Fig. 6, where V' for the $M = 4$ configuration and for the Advanced Toroidal Facility (ATF)[8] vacuum field configuration are plotted. Because the configuration has magnetic shear, at low beta the $M = 4$ configuration should be stable to interchange modes. For these configurations, the potential problems for stability are the ballooning modes.

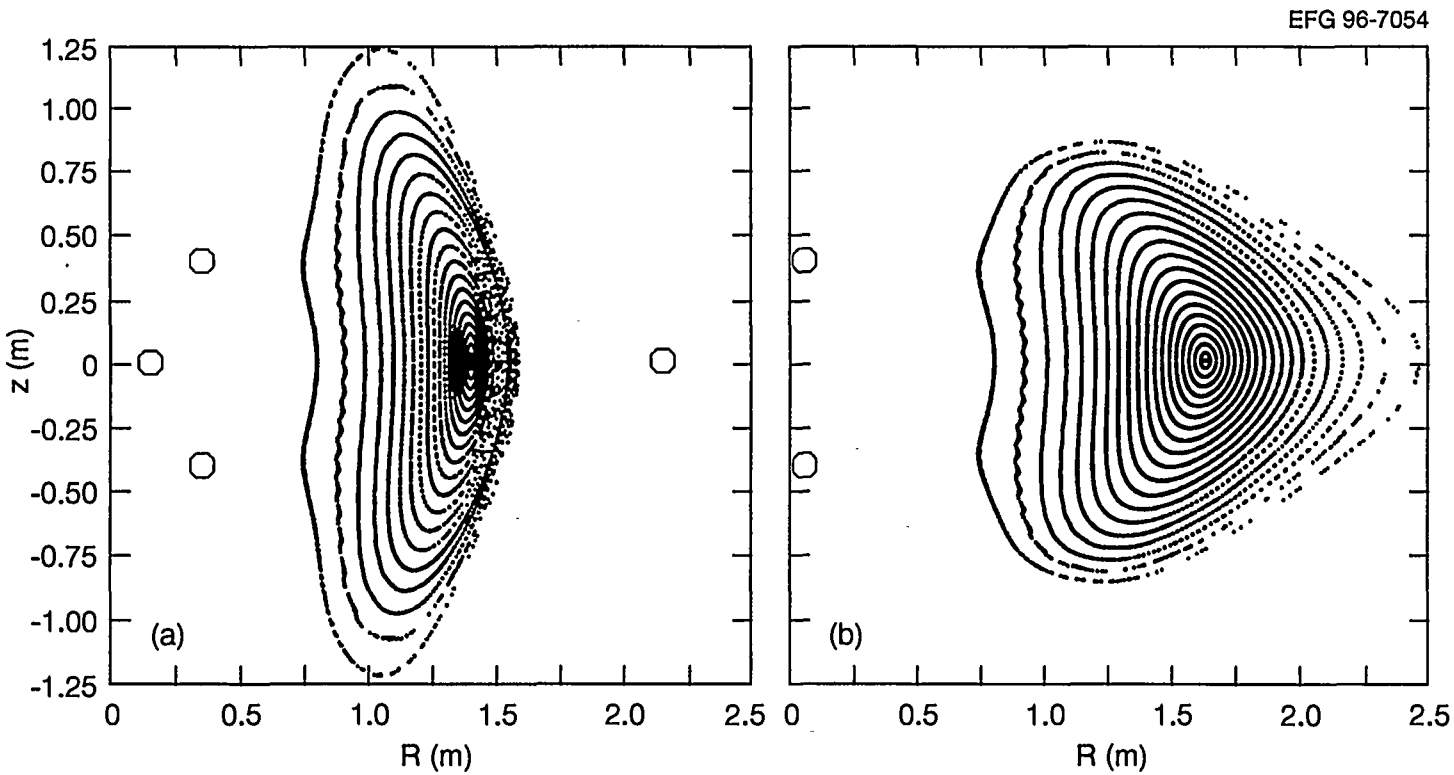

Fig. 3. Vacuum magnetic flux surfaces for an $M = 4$ configuration with A $\approx$ 2.0.

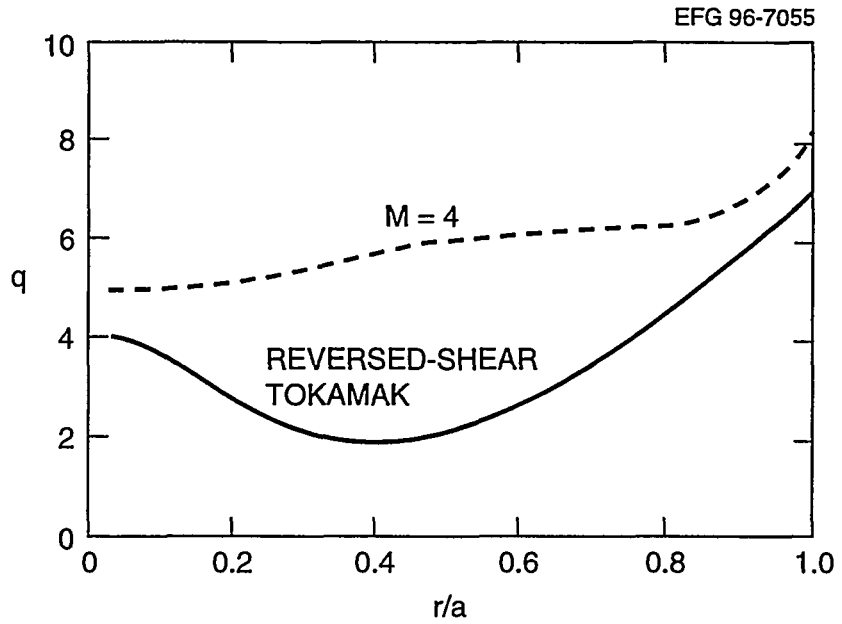

Fig. 4. Rotational transform for the $M = 4$ configuration shown in Fig. 3 and compared with the transform of a typical reversed-shear tokamak configuration.

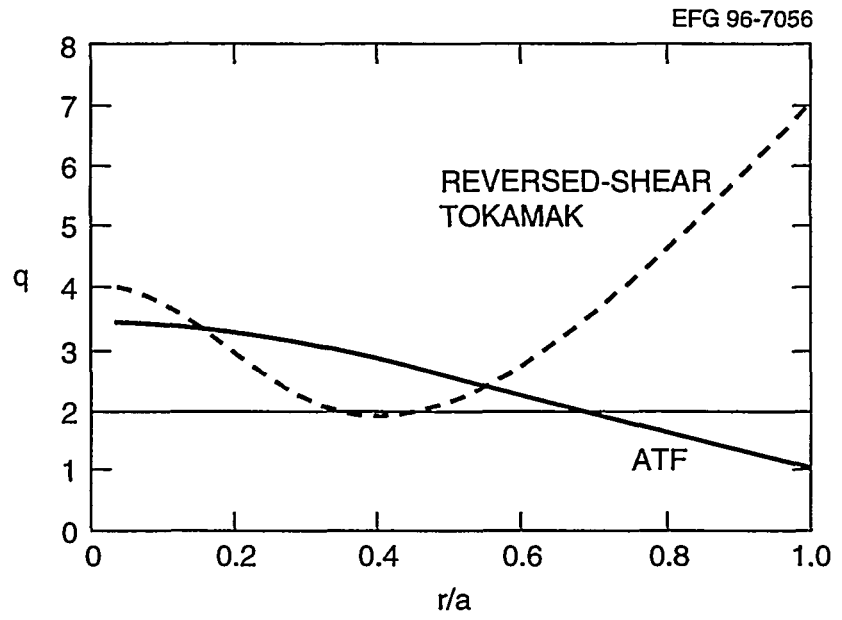

Fig. 5. Rotational transform of the $M = 4$ configuration compared with the ATF rotational transform.

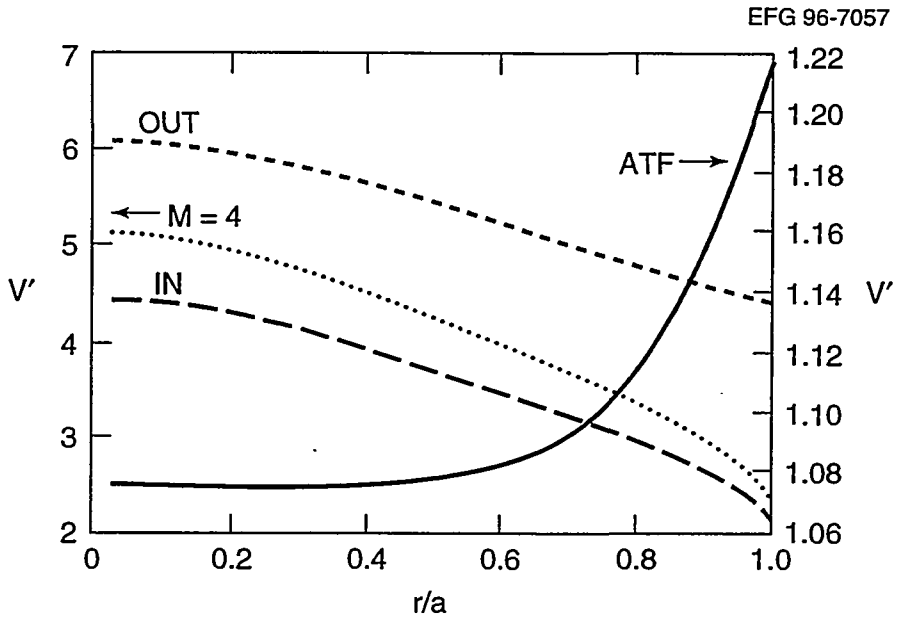

Fig. 6. Radial profile of V' for the $M = 4$ configuration and the corresponding shifted in and out configurations compared to the one for the standard ATF configuration.

4. OPTIMIZATION CRITERIA FOR VACUUM FIELD CONFIGURATIONS

In the process of optimization of the vacuum field configuration we use several criteria, some of them developed from our Compact Torsatron studies.[9] We have already mentioned the more straightforward constraints:

- Transform: tokamaklike with $\iota(0) \approx 0.2$
- $A < 2.5$
- Magnetic well over the whole radius, $V'' < 0$

Other criteria used in the optimization refer to its transport properties. To evaluate the losses in the 1/ν regime, we use the criterion of Shaing and Hokin[10] for a multiple helicity magnetic field, which gives the geometrical factor of the particle flux

$$\Gamma = \int_0^{2\pi} d\theta\, \varepsilon_H(\theta)^{3/2} \left[G_1 \left(\frac{\partial \varepsilon_T}{\partial \theta} \right)^2 - 2G_2 \frac{\partial \varepsilon_T}{\partial \theta} \frac{\partial \varepsilon_H}{\partial \theta} + G_3 \left(\frac{\partial \varepsilon_H}{\partial \theta} \right)^2 \right] . \tag{7}$$

Here $\varepsilon_T(\theta)$ and $\varepsilon_H(\theta)$ are the effective toroidal and helical ripple, respectively, and G_i $(i = 1, 2, 3)$ are numerical coefficients. This criterion has been derived in the

large-aspect-ratio approximation, which is not valid for the present configurations. However, we use this criterion as an indication in the absence of a more accurate one.

For the $M = 4$ configuration, the ripple losses are very high, and Γ is more than an order of magnitude larger than its value for ATF. Furthermore, a second criterion is used in transport optimization for Compact Torsatrons; the maximum area enclosed by the minimum $|B|$ contours is zero for all these configurations. This gives an indication that trapped particles are not confined. Here, we follow a different approach to the particle confinement in the collisionless regime. The recent tokamak results have shown the importance of the creation of internal confinement barriers. They are not only important in suppressing the anomalous transport, but they also reduce the neoclassical transport. The shear electric field modifies the particle orbit through the orbit squeezing factor.[11] This effect has been taken into account for moderate electric field shear but needs to be evaluated for the shear scale length of the order of the ion gyro-radius.

Therefore, we rely on the generation of an electric field shear to reduce the fast particle losses, but at the same time we must reduce the fraction of trapped particles, that is, the magnetic field ripple that is too large for the $M = 4$ configuration.

5. RIPPLE REDUCTION STUDIES

For the $M = 4$ configuration, the addition of four modulated coils at the midfield period position allows the control and reduction of the magnetic field ripple. For this configuration the maximum field ripple is at the magnetic axis, and it is practically zero at the edge. Therefore, we monitor the axis ripple as we change the currents in the four additional coils. The results of this study are shown in Fig. 7. We can see that the ripple on axis is close to 50% for the standard configuration and may be reduced to about 24% with the additional coils. A 24% ripple is still too high. Therefore, we have explored other possible ways of reducing the ripple.

To reduce the ripple it is necessary to increase the number of coils, but we must do so without increasing the aspect ratio beyond 2.5. Two possible approaches are:

- Increasing the number of field periods and having only one coil per field period. To maintain the aspect ratio and the rotational transform at the magnetic axis, we must change the shape of the coils. The best configurations have been found by reducing the ellipticity of the coils and including a moderate triangularity.

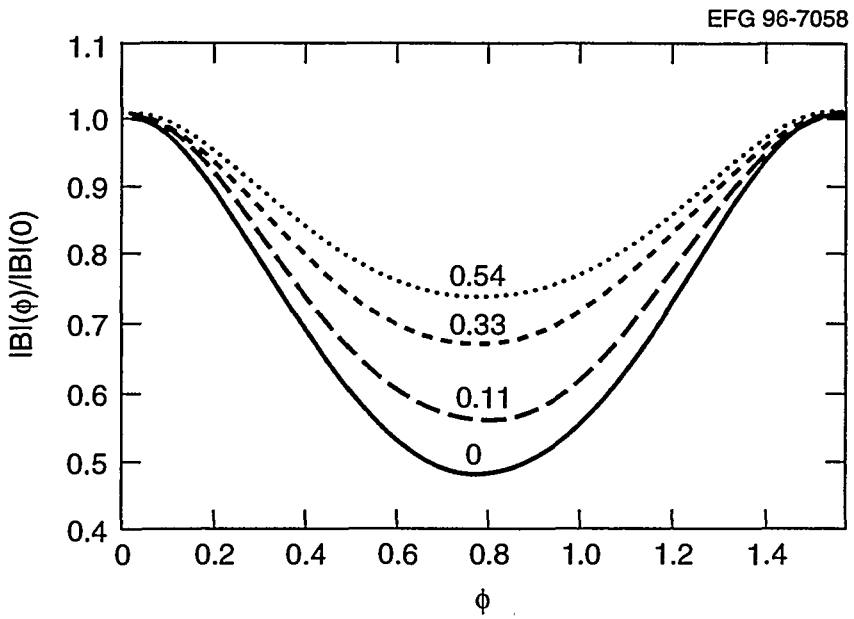

Fig. 7. Ripple on axis for the $M = 4$ configuration and the modification induced by four additional modulated coils.

- Keeping a low number of field periods by increasing the number of coils per field period. In this case, the coils in a field period are no longer equal and they vary in ellipticity and modulation.

Here, we discuss a configuration resulting from each of these approaches. By increasing the number of field periods to 8 and introducing an ellipticity, $e_i = 0.6$, and a triangularity, $\delta_T = 0.45$, a configuration with properties similar to the $M = 4$ configuration was found. The vacuum flux surfaces are shown in Fig. 8. As is shown in Fig. 9, by changing the position of the magnetic axis, the sizes of the vacuum flux surfaces and the rotational transform change. When the magnetic axis position is between 1.5 and 1.6, the aspect ratio is about 2.3 and the transform is close to that of the $M = 4$ configuration.

An example of the second approach is an $M = 2$ configuration with eight coils per field period. The vacuum flux surfaces are shown in Fig. 10. For this configuration the ellipticity varies with the coil from 0.5 to 1.5, and the triangularity is zero. The aspect ratio is 2.2, and the rotational transform at the magnetic axis is about 0.1, somewhat lower than our stated goal. If the number of coils per field period is between five and eight, there is not much change in the size of the vacuum flux surfaces nor in the axis rotational transform (Fig. 11). Both the $M = 8$ configuration and the $M = 2$ configuration with 16 coils have reduced the ripple. In the case of the $M = 2$ configuration, the ripple is lower than the value for ATF (Fig. 12).

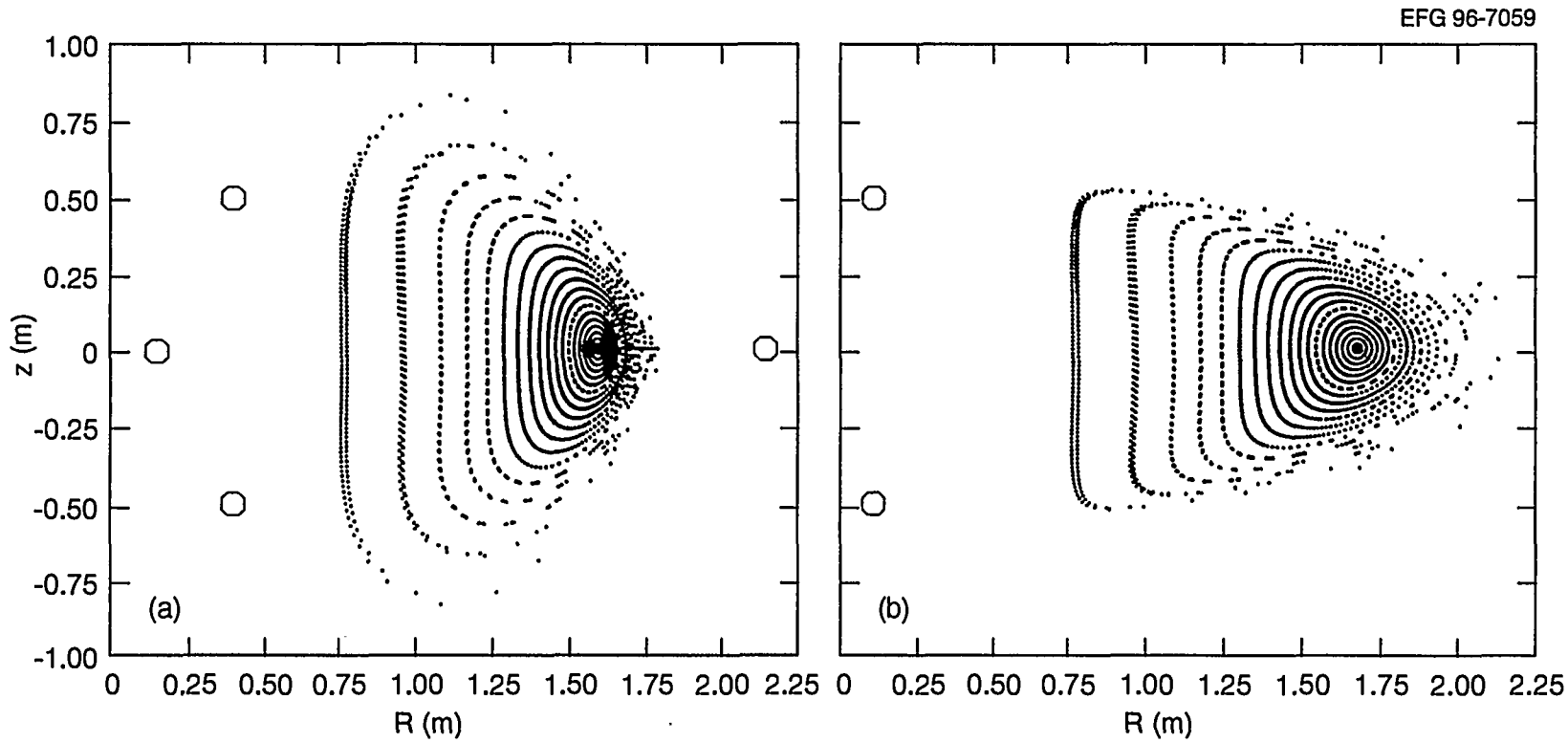

Fig. 8. Vacuum flux surfaces for an $M = 8$ configuration with modulated and shaped coils.

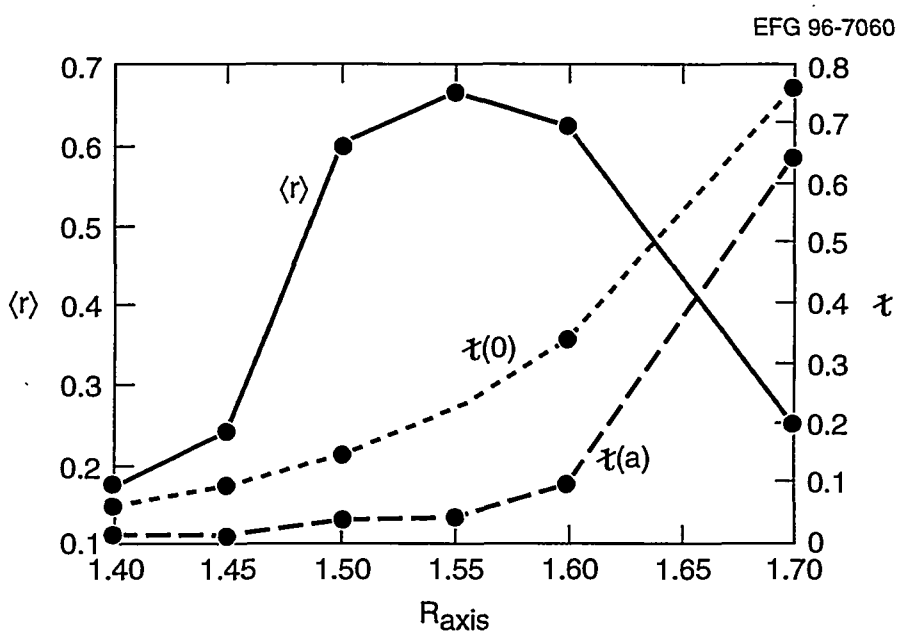

Fig. 9. Averaged radius of the last flux surface and rotational transform for the $M = 8$ configuration of Fig. 8 as a function of the magnetic axis position.

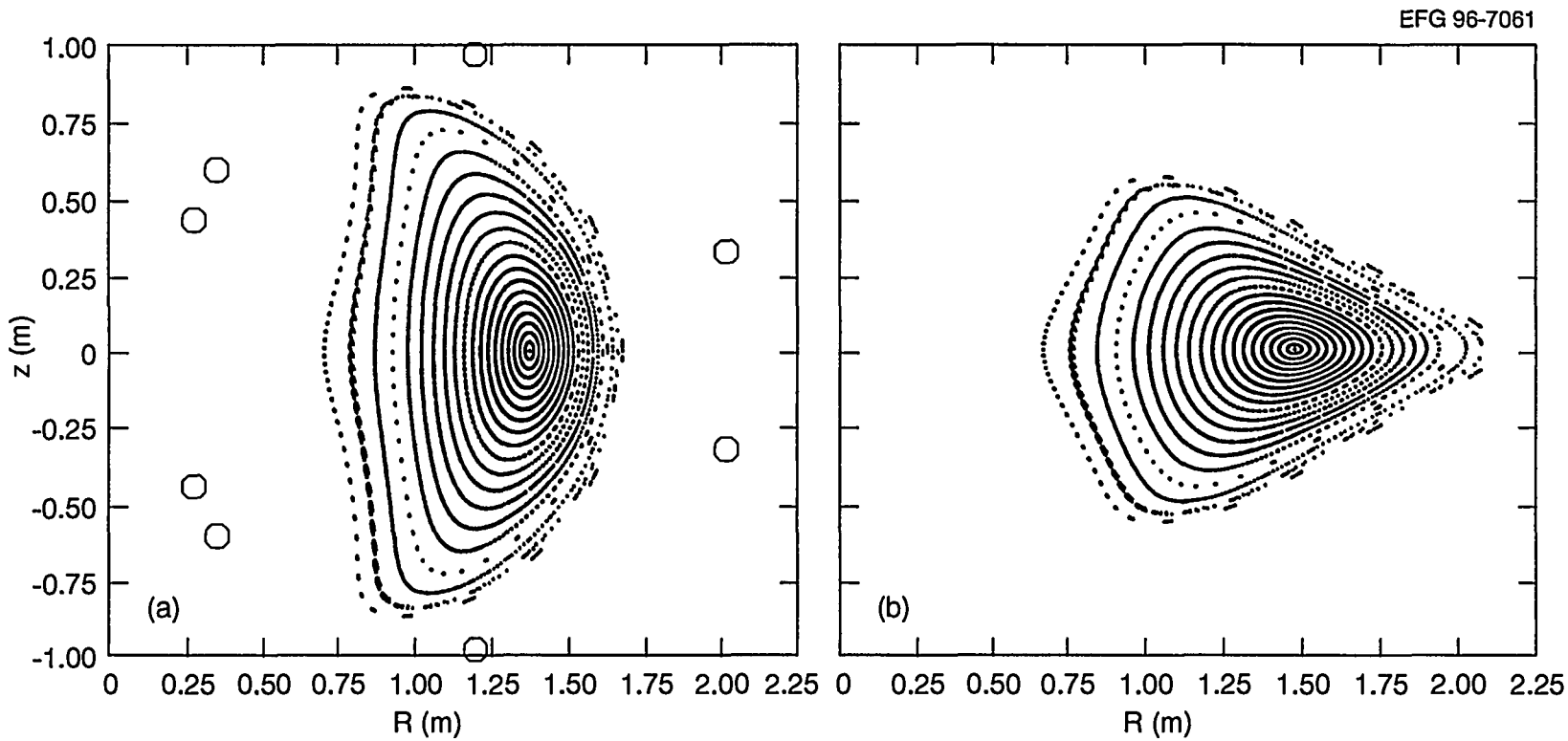

Fig. 10. Vacuum flux surfaces for an $M = 2$ configuration with 8 coils per field period.

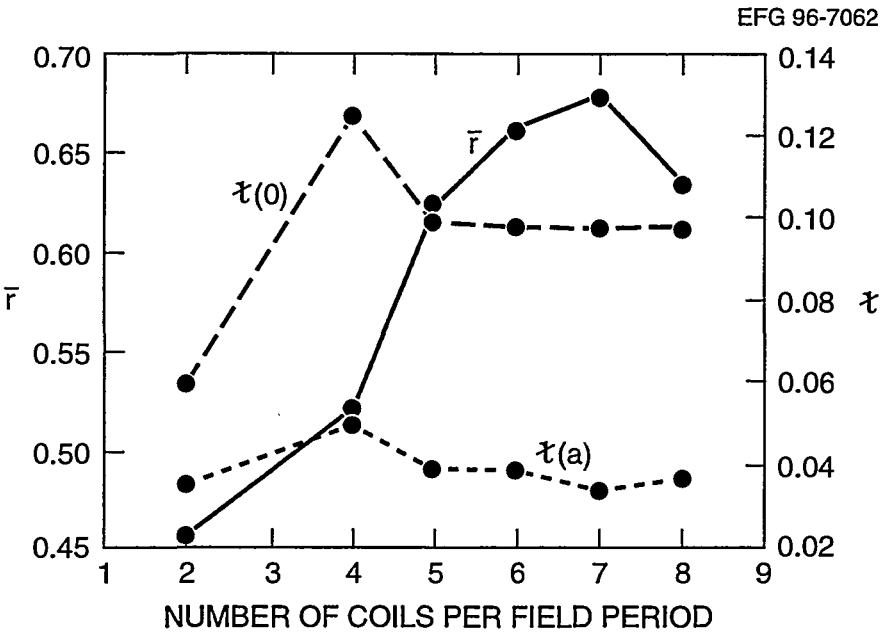

Fig. 11. Averaged radius of the last flux surface and rotational transform for an $M = 2$ configuration as a function of the number of coils per field period.

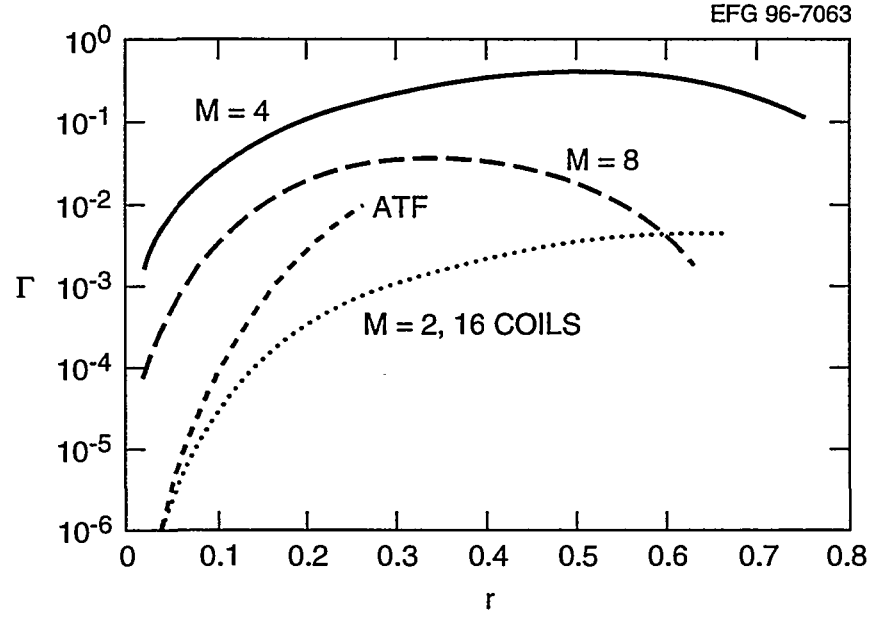

Fig. 12. Geometrical factor of the particle flux, Eq. (7), for the different configurations studied correspond to ATF.

6. CONCLUSIONS

The use of modulated coils offers a new path to the tokamak-stellarator hybrids. Low-aspect-ratio configurations can be found with robust vacuum flux surfaces and rotational transform close to a reversed-shear tokamak. They have clear advantages:

- Very low toroidal currents are needed. Hence, the disruption problems are minimized, and the existence of vacuum flux surfaces may ameliorate their effects.
- They considerably reduce the current drive needs.
- The magnetic configuration does not require linked toroidal coils.

For a hybrid tokamak-stellarator to have a competitive confinement, control of electric field shear is needed. We must investigate the effectiveness of electric field shear on the confinement of the energetic particles and its impact on neoclassical transport.

ACKNOWLEDGMENTS

Valuable discussions with D. B. Batchelor, R. J. Colchin, C. L. Hedrick, J. N. Leboeuf, J. F. Lyon, and P. K. Mioduszewski are gratefully acknowledged. We would like to thank Oak Ridge National Laboratory, managed by Lockheed Martin Energy Research Corporation for the U.S. Department of Energy under contract number DE-AC05-96OR22464, for funding the research for the Small-Aspect-Ratio Toroidal Hybrid Device through the Laboratory's Seed Money Program.

REFERENCES

1. B. A. Carreras et al., *Nucl. Fusion* **28**, 1195 (1988).
2. T. K. Chu et al., *IEEE Trans. Plasma Sci.* **9**, 228 (1981).
3. J. F. Lyon et al., "Stellarator Physics Evaluation Studies" in *Proceedings of the Ninth Intl. Conf. on Plasma Physics and Controlled Nuclear Fusion Research* (International Atomic Energy Agency, Vienna, 1983), Vol. 3, p. 115.
4. V. E. Bykov et al., "Optimization Studies of Compact Torsatrons" in *Proceedings of the Twelfth Intl. Conf. on Plasma Physics and Controlled Nuclear Fusion Research* (International Atomic Energy Agency, Vienna, 1989), Vol. 2, p. 403.
5. P. Moroz, *Phys. Plasmas* **2**, 4267 (1995).
6. B. A. Carreras et al., *Nucl. Fusion* **24**, 1347 (1984).
7. G. Griger et al., *Nucl. Fusion* **25**, 1231 (1984).
8. J. F. Lyon et al., *Fusion Technol.* **10**, 179 (1986).
9. B. A. Carreras et al., *Confinement Improvement of Low-Aspect-Ratio Torsatrons*, ORNL/TM-11101, Martin Marietta Energy Systems, Inc., Oak Ridge National Laboratory, 1989.
10. K. C. Shaing and S. A. Hokin, *Phys. Fluids* **26**, 2136 (1983).
11. K. C. Shaing and R. D. Hazeltine, *Phys. Fluids B* **4**, 2547 (1992).

ORNL/TM-13252
Dist. Category UC-427

INTERNAL DISTRIBUTION

1. D. B. Batchelor
2. L. A. Berry
3-12. B. A. Carreras
13. R. J. Colchin
14. S. P. Hirshman
15. J. T. Hogan
16. W. A. Houlberg
17. J. N. Leboeuf
18. R. P. Leinius
19. V. E. Lynch
20. J. F. Lyon
21. S. L. Milora
22. P. K. Mioduszewski
23. M. Murakami
24. D. E. Newman
25. J. A. Rome
26. M. J. Saltmarsh
27. D. A. Spong
28. A. Ware
29-30. Laboratory Records Department
31. Laboratory Records, ORNL-RC
32. Central Research Library
33. Document Reference Section
34. Fusion Energy Division Library
35. ET/FE Division Publications Office
36. ORNL Patent Office

EXTERNAL DISTRIBUTION

37. Office of the Assistant Manager for Energy Research and Development, Department of Energy Field Office, Oak Ridge, P.O. Box 2000, Oak Ridge, TN 37831
38. N. A. Davies, Associate Director for Fusion Energy Sciences, Office of Energy Research, (ER-50), DOE, 19901 Germantown Road, Germantown, MD 20874-1290
39. M. Roberts, Office of Fusion Energy Sciences, Office of Energy Research (ER-52), DOE, 19901 Germantown Road, Germantown, MD 20874-1290
40. D. E. Baldwin, General Atomics, 13-216A, P.O. Box 85608, San Diego, CA 92186-9784
41. R. W. Conn, University of California at San Diego, School of Engineering, 9500 Gilman Drive, La Jolla, CA 92093-0403
42. D. J. Sigmar, Director, Plasma Fusion Center, NW 16-202, Massachusetts Institute of Technology, Cambridge, MA 02139
43. K. I. Thomassen, Lawrence Livermore National Laboratory, P.O. Box 5511, Livermore, CA 94550
44. J. D. Callen, Department of Nuclear Engineering, University of Wisconsin, Madison, WI 53706-1687
45. S. O. Dean, Fusion Power Associates, 2 Professional Drive, Suite 248, Gaithersburg, MD 20879
46. H. K. Forsen, Bechtel Group, Inc. Research Engineering P. O. Box 3965, San Francisco, CA 94105
47. R. W. Gould, Department of Applied Physics California Institute of Technology Pasadena, CA 91125
48. R. J. Hawryluk, Princeton Plasma Physics Laboratory, P.O. Box 451, Princeton, NJ 08543
49. D. M. Meade, Princeton Plasma Physics Laboratory, P.O. Box 451, Princeton, NJ 08543
50. W. M. Stacey, School of Nuclear Engineering and Health Physics, Georgia Institute of Technology, Atlanta, GA 30332

51. D. Steiner, Nuclear Engineering Department, NES Building, Tibbetts Avenue, Rensselaer Polytechnic Institute, Troy, NY 12181
52. Bibliothek, Max-Planck Institut für Plasmaphysik, Boltzmannstrasse 2, D-85748 Garching, Germany
53. Bibliothek, Institut für Plasmaphysik, KFA Jülich GmbH, Postfach 1913, D-5170 Jülich, Germany
54. Bibliothek, KfK Karlsruhe GmbH, Postfach 3640, D-7500 Karlsruhe 1, Germany
55. Bibliotheque, Centre de Recherches en Physique des Plasmas, Ecole Polytechnique Fédérale de Lausanne, 21 Avenue des Bains, CH-1007 Lausanne, Switzerland
56. R. Aymar, CEN/Cadarache, Departement de Recherches sur la Fusion Controlee {F-13108}, Saint-Paul-lez-Durance, Cedex, France
57. Bibliothèque, CEA/Cadarache, F-13108, Saint-Paul-lez-Durance, Cedex, France
58. Library, JET Joint Undertaking, Abingdon, Oxfordshire OX14 3EA, England
59. Library, FOM-Instituut voor Plasmafysica, Rijnhuizen, Edisonbaan 14, 3439 MN Nieuwegein, The Netherlands
60. Library, National Institute for Fusion Science, Chikusa-ku, Nagoya 464-01, Japan
61. Library, International Centre for Theoretical Physics, P.O. Box 586, I-34100 Trieste, Italy
62. Library, Centro Richerche Energia Frascati, C.P. 65, I-00044 Frascati (Roma), Italy
63. Library, Plasma Physics Laboratory, Kyoto University, Gokasho, Uji, Kyoto 611, Japan
64. Plasma Research Laboratory, Australian National University, P.O. Box 4, Canberra, A.C.T. 2601, Australia
65. Library, Japan Atomic Energy Research Institute, Naka Fusion Research Establishment, 801-1 Mukoyama, Naka-machi, Naka-gun, Ibaraki-ken, Japan
66. G. A. Eliseev, I. V. Kurchatov Institute of Atomic Energy, P.O. Box 3402, 123182 Moscow, Russia
67. V. A. Glukhikh, Scientific-Research Institute of Electro-Physical Apparatus, 188631 Leningrad, Russia.
68. I. Shpigel, Institute of General Physics, Russian Academy of Sciences, Ulitsa Vavilova 38, Moscow, Russia
69. O. Pavlichenko, Kharkov Physical-Technical Institute, Academical St. 1, 310108 Kharkov, Ukraine
70. Deputy Director, Southwestern Institute of Physics, P.O. Box 15, Leshan, Sichuan, China (PRC)
71. Director, Institute of Plasma Physics, P.O. Box 26, Hefei, Anhui, China, (PRC)
72. R. H. McKnight, Office of Energy Research, ER-542, 19901 Germantown Road, Germantown, MD 20874
73. E. Oktay, Office of Fusion Energy Sciences, Office of Energy Research (ER-55), DOE, 19901 Germantown Road, Germantown, MD 20874-1290
74. W. Sadowski, Office of Fusion Energy, Office of Energy Research, ER-541, 19901 Germantown Road, Germantown, MD 20874-1290
75. M. N. Rosenbluth, ITER Co-Center, 11025 North Torrey Pines Road, San Diego ITER Site, La Jolla, CA 92037
76. Duk-In Choi, Department of Physics, Korea Advanced Institute of Science and Technology, P.O. Box 150, Chong Ryang-Ri, Seoul, Korea
77. Library of the Physics Department, University of Ioannina, Ioannina, Greece

78. C. De Palo Library, Associazione EURATOM-ENEA sulla Fusione, C.P. 65, Frascati (Roma), Italy
79. Laboratorio Associado de Plasma, Instituto Nacional de Pesquisas Espaciais, Caixa Postal 515, 122201, Sao Jose doe Campos, SP, Brazil
80. Theory Department Read File, c/o R. Hazeltine, University of Texas Institute for Fusion Studies Austin, TX 78712
81. Theory Department Read File, c/o D. J. Sigmar, Director Plasma Fusion Center, NW 16-202, Massachusetts Institute of Technology, Cambridge, MA 02139
82. Theory Department Read File, c/o W. Tang, Princeton Plasma Physics Laboratory, P.O. Box 451, Princeton, NJ 08544
83. Theory Department Read File, c/o L. Kovrizhnykh, Lebedev Institute of Physics, Academy of Sciences, 53 Leninsky Prospect, 117924 Moscow, Russia
84. Theory Department Read File, c/o B. B. Kadomtsev, I. V. Kurchatov Institute of Atomic Energy, P.O. Box 3402, 123182 Moscow, Russia
85. Theory Department Read File, c/o T. Kamimura, National Institute of Fusion Science, Nagoya University, Nagoya~464, Japan
86. Theory Department Read File, c/o E. Maschke, Departemente de Recherches sur la Fusion Controlée, CEN/Cadarache, F-13108 Saint-Paul-lez Durance, France
87. Theory Department Read File, c/o D. Düchs, JET Joint Undertaking, Culham Laboratory, Abingdon, Oxfordshire, OX14 3EA England
88. Theory Department Read File, c/o R. Briscoe, Culham Laboratory, Abingdon, Oxfordshire OX14 3DB England
89. Theory Department Read File, c/o D. Biskamp, Max-Planck-Institut für Plasmaphysik, Boltzmannstrasse 2, D-8046 Garching, Federal Republic of Germany
90. Theory Department Read File, c/o T. Takeda, Japan Atomic Energy Research Institute, Tokai Establishment, Tokai-mura Naka-gun Ibaraki-ken, Japan
91. Theory Department Read File, c/o R. Waltz, General Atomics, P.O. Box 81608, San Diego, CA 92138
92. Theory Department Read File, c/o R. Cohen, L-630 Lawrence Livermore National Laboratory, P.O. Box 5511, Livermore, CA 94550
93. Theory Department Read File, c/o D. Burnes, CTR Division, Los Alamos National Laboratory, P.O. Box, 1663, Los Alamos, NM 87545
94-95. Given distribution as shown in DOE/OSTI-4500-R75 under category UC-427